J Mater Sci: Mater Med (2007) 18:399–404
DOI 10.1007/s10856-006-0705-6

The effects of nanoscale pits on primary human osteoblast adhesion formation and cellular spreading

M. J. P. Biggs · R. G. Richards · N. Gadegaard · C. D. W. Wilkinson · M. J. Dalby

Received: 16 June 2006 / Accepted: 25 September 2006

Abstract Current understanding of the mechanisms involved in ossesoinegration following implantation of a biomaterial has led to an emphasis being placed on the modification of material topography to control interface reactions. Recent studies have inferred nanoscale topography as an important mediator of cell adhesion and differentiation. Biomimetic strategies in orthopaedic research aim to exploit these influences to regulate cellular adhesion and subsequent bony tissue formation. Here experimental topographies of nanoscale pits demonstrating varying order have been fabricated by electron-beam lithography in (poly)carbonate. Osteoblast adhesion to these nanotopographies was ascertained by quantification of the relation between adhesion complex formation and total cell area. This study is specifically concerned with the effects these nanotopographies have on adhesion formation in S-phase osteoblasts as identified by BrdU incorporation. Nanopits were found to reduce cellular spreading and adhesion formation.

1 Introduction

Topographical modification of a device intended for *in vivo* use may be viewed as a potential strategy to confer favourable tissue integration at the cell-biomaterial interface. Fracture fixation, and prosthesis implantation rely on controlled osseointegration to regulate cellular adhesion and improve implant stability. Substrate microroughness is associated with increased cell adhesion [1], often deemed unfavourable for internal fixation devices that are destined for future removal. Adhesion of mineralised tissue increases the force required for nail or screw extraction [2, 3], which can be associated with local bone fracture upon removal [4]. Conversely long-term implants must in parts promote cellular adhesion and osseointegration to prevent aseptic loosening and subsequent device failure [3].

Once implanted, an *in vivo* device is immediately subjected to the adsorption of plasma constituents [5]. Cellular adhesion to a biomaterial is mediated by cell adhesion molecules (CAMs) coupled to specific motifs present in extracellular matrix (ECM) molecules. Integrins, a subset of these CAMs, are responsible for the intracellular assembly of adhesion complexes and the recruitment of proteins involved in cell adhesion and adhesion plaque formation. These adhesion complexes contain structural and also secondary signalling molecules crucial to cell adhesion and function and thus act as mediators between the ECM and cell cytoskeleton. Integrin receptors are activated following interactions with the ECM and cluster in the plasma membrane. As internalor external stresses are applied to membrane associated integrins, intracellular transduction responses can lead to further adhesion assembly and cytoskeletal organisation [6].

A highly ordered hierarchical recruitment of focal adhesion associated proteins occurs during focal adhesion complex assembly. Many of the constituent proteins are still unknown but most important for cell structure and stability are the cytoskeletal-associated proteins [7]. Vinculin is a plasma membrane associated protein found in adhesion complexes and involved in the coupling of the actin-based

M. J. P. Biggs (✉) · N. Gadegaard · C. D. W. Wilkinson · M. J. Dalby
Centre for Cell Engineering, Institute of Biomedical and Life Sciences, Joseph Black Building, University of Glasgow, Glasgow, G12 8QQ, UK
e-mail: m.biggs.1@research.gla.ac.uk

M. J. P. Biggs · R. G. Richards
AO Research Institute, AO Foundation, Clavadelerstrasse 8, Davos Platz, Switzerland

microfilaments to the adhesion plaque [8]. It is one of the most prominent proteins of the adhesion complex and binds to a number of other adhesion associated proteins, facilitating the assembly of the adhesion site [7]. Vinculin is present in a number of adhesion subtypes and can therefore be used as an ideal marker protein to label integrin-associated adhesions subtypes.

Nanotechnology derived from the microelectronics industry has facilitated the development of nanoscale topographical manipulation, and the fabrication of highly controlled experimental substrates for adhesion assays [9, 10]. These devices can be used to directly evaluate effects of nanoscale topography on cellular adhesion. Experimentally, nanogrooves [11], nanopits [12], and nanoislands [13] have been shown to affect contact guidance *in vitro* and directly influence cellular behaviour. Nanoscale influence may have its origins in disrupting the formation of adhesion sites, by acting as initial promoters of cellular adhesion, or by influencing differentiation and function.

This study is concerned with the influence of nanoscale pits on adhesion formation in primary human osteoblasts (HOBs). S-phase cells were identified by Bromodeoxyuridine (BrdU) incorporation, and subsequent fluorescent labelling. We focused on cells in S-phase as these have been shown earlier to exhibit increased substrate flattening, and because S-phase has also been associated with a reduced intercell variation in adhesion numbers [14]. To quantify adhesion sites, and visualise cytoskeletal elements vinculin and actin were immuno-labelled and visualised by fluorescent microscopy.

2 Materials and methods

2.1 Nano patterning and die fabrication

Samples were made in a three-step process of electron beam lithography (EBL), nickel die fabrication and injection moulding. Silicon substrates were coated with ZEP 520A (Zeon corporation) resist to a thickness of 100 nm. Samples were baked for a 1–2 h at 180°C prior to exposure in a Leica EBPG 5-HR100 beamwriter at 50 kV. Arrays of pits in random (Rand) and square (Sq) conformations were fabricated. An 80 nm spot size was used, resulting in pits 100 nm deep with a diameter of 120 nm. The pitch between the Square arrays of pits was 300 nm. After exposure the samples were developed in xylene at 23°C for 60 sec and rinsed in copious amounts of propan-2-ol before being blown dry with filtered nitrogen. For more information about the procedure see [15].

Nickel dies were made directly from the patterned resist samples. A thin (50 nm) layer of Ni-V was sputter coated on the samples. That layer acted as an electrode in the subsequent electroplating process. The dies were plated to a thickness of ca. 300 nm. For more information about the procedure see [16].

Polymeric replicas were made in DVD grade (poly)carbonate (PC) (Macrolon DP1-1265, Bayer) by injection moulding. PC was used as it is known to have very good replication capabilities [17]. Subsequent injection moulded replicas possessed a central nano-imprinted area of 1 cm^2.

2.2 Cell culture

Primary human osteoblasts (HOBs) were obtained from PromoCell® (Heidelberg, Germany), these were derived from human hipbone biopsies, and were cultured according to PromoCell® guidelines. Cells were cultured in 75 cm^2 flasks in an osteoblast growth medium (OGM) encompassing 10% foetal calf serum supplied by PromoCell®. Culture medium was free of antibiotics. Experimental substrates were sterilized by three sequential 5-second immersions in 70% ethanol followed by 2 sequential 5-second immersions in HEPES (N-(2-hydroxyethyl)-piperazine-N'-2-ethanesulfonic acid) buffer, pH 7.4.

Cells were cultured for 10 days in 75 cm^2 flasks, before trypsinisation, and seeding onto planar control, and nanopatterned substrates at a density of 1×10^4 cells per sample in 2 ml of complete medium. HOBs were incubated at 37°C with a 5% CO_2 atmosphere and OGM replaced twice weekly. Following 6 days of culture HOBs were maintained for 4 days without being supplemented with fresh medium. This induced a brief period of serum starvation. Serum rich media was subsequently introduced to the culture, and cells allowed to metabolise for 17 hours, giving rise to a population of cells possessing a synchronised nuclear cycle [18]. Following this period the cells were cultured in 10 μM BrdU/OGM for 3 hours.

2.3 Immunofluorescent labelling

HOBs were fixed in 4% formaldehyde in Phosphate buffered solution (PBS), with 1% sucrose at 37°C, pH 7.4 for 15 min. Once fixed, the samples were washed with PBS. Samples were permeabilised with buffered 0.5% Triton X-100 within a buffered isotonic solution (10.3 g sucrose, 0.292 g NaCl, 0.06 g $MgCl_2$, 0.476 g HEPES buffer, 0.5 ml Triton X 100, in 100 ml water, pH 7.2) at 4°C for 5 min. Non-specific binding sites were blocked with 1% bovine serum albumin (BSA) in PBS at 37°C for 5 min and subsequently incubated for 2 hours with a 1:200 concentration anti-vinculin (monoclonal anti-human raised in mouse, clone hVin-1; IgG1, Sigma, Poole, UK) followed by incubation in 1:100 concentration of anti-BrdU/DNase solution for 1 h (37°C) (RPN2001, Amersham Biosciences cell proliferation kit, Uppsala, Sweden). Simultaneously, rhodamine

conjugated phalloidin was added for the duration of this incubation (1:100 in 1% BSA/PBS, Molecular Probes, Oregon, USA). Non-specific charges (e.g. remaining aldehyde) were neutralised with 0.5% Tween 20/PBS (5 min ×3) to minimise background labelling. A secondary, biotin conjugated antibody, (1:50 in 1% BSA/PBS, monoclonal horse anti-mouse (IgG), Vector Laboratories, UK) was added for 1 h (37°C) followed by subsequent washing as above. A Fluorescein conjugated streptavidin third layer was added (1:50 in 1% BSA/PBS, Vector Laboratories, UK) at 4°C for 30 min, and given a final wash. Samples were mounted in Vectorshield mountant for fluorescence imaging (Vector Laboratories, UK), and then viewed with a Zeiss Axiovert 200M microscope with a Zeiss Plan Neofluor 40× (0.75 NA) lens. Image manipulation in Adobe® Photoshop was then used to transpose the colour layers to show adhesion complexes (vinculin) in green, actin in red and S-phase nuclei in blue.

2.4 Image analysis

For adhesion quantification Image J was used (downloaded from the National Institute of Health, Bethesda, MD, USA, free download available at http://rsb.info.nih.gov/ij/) [19]. This used automated detection of total cell area and vinculin labelling of which approximately 20 S-phase cells were analysed on each material from two material replicates. Total adhesion area was quantified and expressed as a percentage of total cell area.

2.5 Statistics

Data was $\log_2$ normalised and analysed using Tukey ANOVA. Results of $p < 0.05$ were considered significant (differences $p < 0.05$ denoted by $\star$, $p < 0.01$ denoted by $\star\star$).

3 Results

3.1 Characterisation of substrate topography

Nanopit substrates fabricated by injection moulding were examined by scanning electron microscopy. Nanoscale pits were all 120 nm in diameter, and 100 nm deep (Fig. 1(A) and (B)). Two types of nanofeatured surfaces were produced: 'Rand' substrates possessed randomly distributed pits, resulting in a clustering of nanotopographical features as well as extended areas of planar substrate. 'Sq' substrates had nanopit on a square lattice, with a pitch of 300 nm. The patterned substrate area measured 1 cm^2. Material pit coverage was quantified as 'Sq' and 'Rand' possessing approximately the same number of pits per area. Planar PC controls had an average Ra of 1.17 nm over 10 μm.

3.2 HOB cytoskeletal organisation and adhesion localisation

S-phase HOBs cultured on planar controls were well spread and formed numerous adhesion complexes at the cell periphery and the perinuclear region. The cell cytoskeleton was well developed and F-actin bundles formed large contractile stress fibres. Adhesion complexes were predominantly dash shaped, and intimately associated with the cell cytoskeleton, located at the perinuclear and peripheral regions (Fig. 2(A)).

HOBs cultured on 'Rand' nanoarrays appeared well spread with well-developed cytoskeletal elements. Cells possessed large elongated adhesions in conjunction with prominent stress fibre formation. Adhesion formation was localised predominantly to the cell periphery, yet they were not observed to be involved in lamellapodial extensions (Fig. 2(B)).

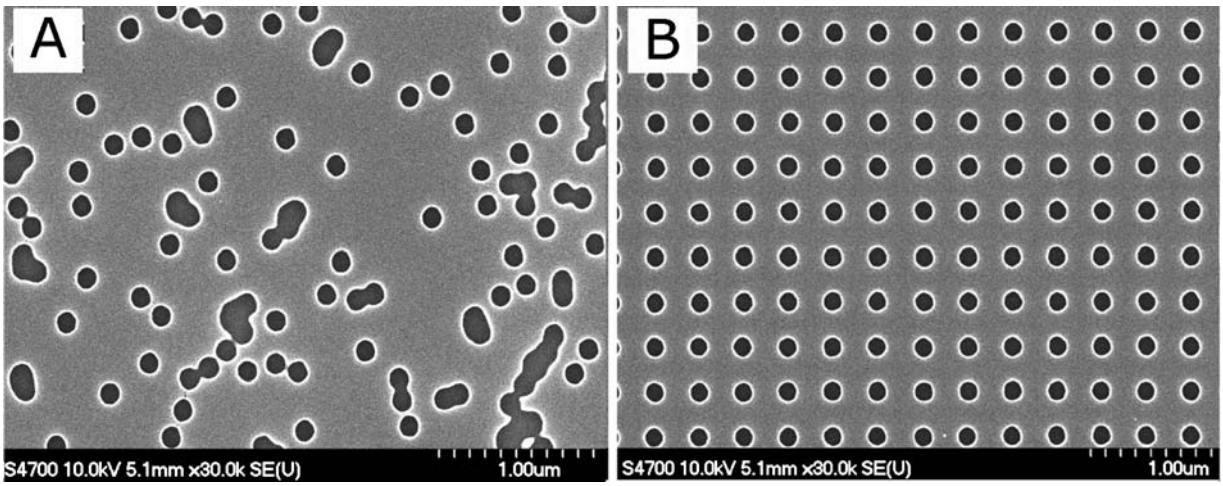

Fig. 1 *SEM image of experimental substrates: Nanopit arrays in polycarbonate*. (A) 'Rand' nanopit arrays resulted in planar areas with no pits present and areas of large irregular pits formed by clustering of multiple pits. (B) 'Sq' substrates possessed highly ordered conformations of nanoscale pits. Pitch, pit diameter and depth were maintained throughout the imprinted surface

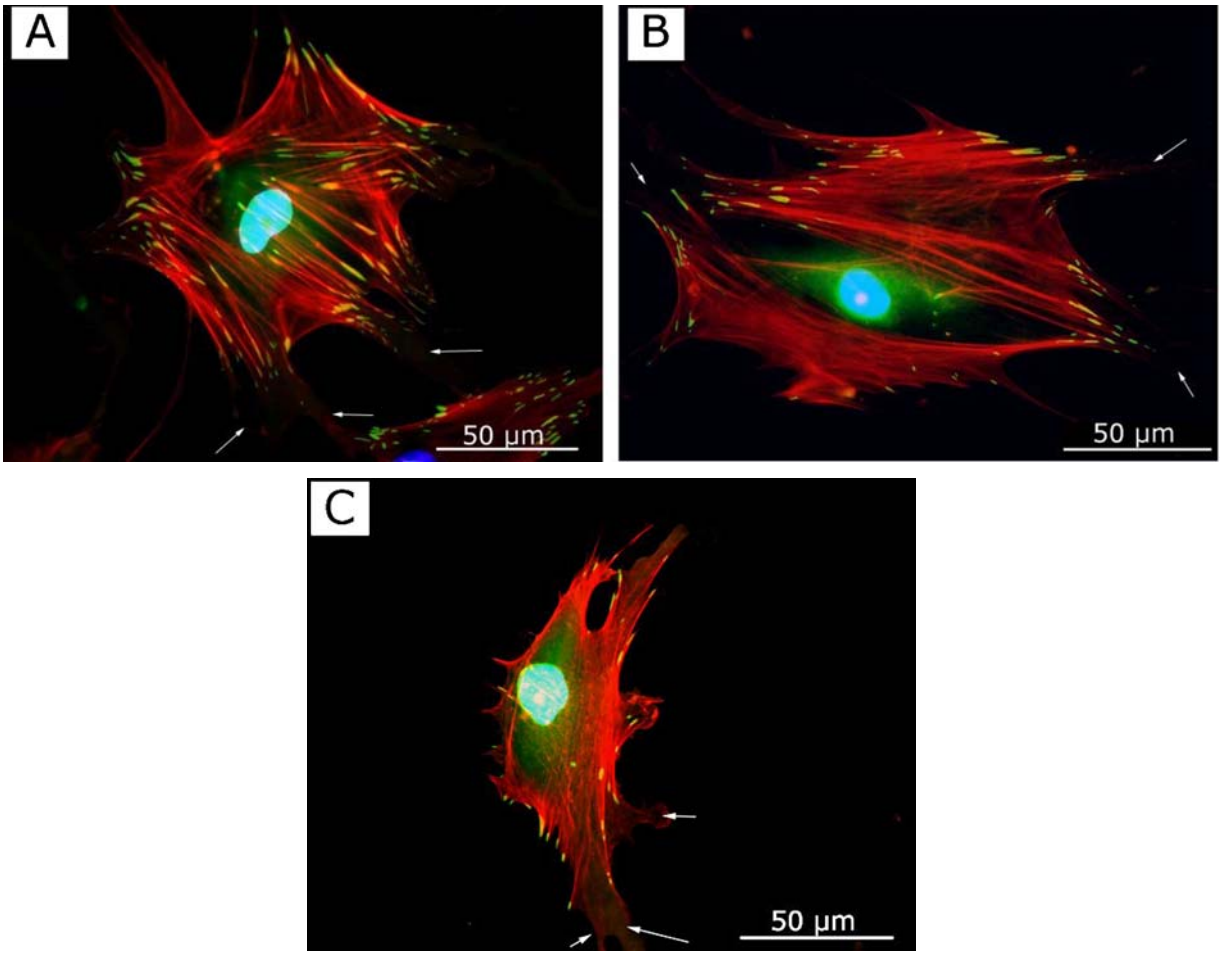

Fig. 2 *Fluorescent Microscopy Image of S-phase HOBs cultured on nanopit substrates*. Nanopits effected adhesion formation, cell spreading and cytoskeletal organisation. BrdU positive nuclei blue, vinculin green, and actin red. (A) HOBs cultured on control substrates were well spread and formed multiple large adhesion complexes and mature organised stress fibres. (B) Random arrays of nanopits induced cellular spreading and stress fibre organisation, however adhesion formation was reduced. (C) Square arrays of nanopits perturbed cytoskeletal organisation and stress fibre development. Cellular spreading was disrupted and adhesion formation reduced. Red = actin, Light blue = S-phase nuclei, Dark blue = non S-phase nuclei, Green = vinculin. Lamellapodia = white arrows

HOBs cultured on 'Sq' nanopit arrays possessed a relatively less spread morphology and exhibited perturbed cytoskeletal formation. Again, adhesion formation was restricted to peripheral regions yet they were not observed to be involved in lamellapodial extensions (Fig. 2(C)).

3.3 Total adhesion area

Adhesion complex formation in HOBs cultured on control substrates occupied approximately 2.3% of the total cell area. Well spread cells were associated with numerous large adhesions, while less spread cells possessed fewer adhesion complexes.

Both experimental substrates resulted in reduced adhesion numbers in S-phase HOBs relative to planar controls. S-phase HOBs cultured on nanopit substrates were associated with a diminished total area of cell adhesion. Adhesion numbers were reduced in HOBs cultured on 'Rand' nanoarrays, this reduction however was not associated with an appreciable decline in cell area. HOBs cultured on 'Sq' substrates underwent a reduction in adhesion formation coupled with reduced total cell area. Adhesion area was 1% of the total cell area approximately 50% of that observed in HOBs cultured on planar controls (Fig. 3).

4 Discussion

Topographical modification of an orthopaedic implant may be a viable method to guide tissue integration, as it has been shown *in vitro* to dramatically influence osseogenesis, inhibit bone resorbtion [20, 21], and prevent cell adhesion [22]. Non-adhesive surface modification is of great potential benefit in the design of orthopaedic implants, in particular where internal fixation devices have been reported to induce latent

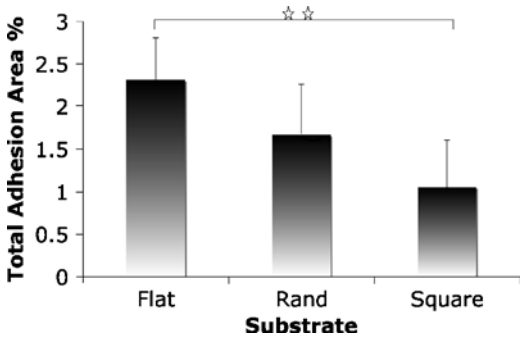

Fig. 3 *Total cell area occupied by adhesion complexes in HOBs cultured on nanopit substrates.* Adhesion area on flat substrates was approximately 2.3% of the cellular spreading area. The relative area of adhesions was reduced on both the nanopitted substrates; HOBs cultured on 'Rand' and 'Sq' substrates exhibited approximately 1.6% and 1% total adhesion coverage respectively. Results are ± Standard deviation. Differences $p < 0.01$ denoted by ⋆⋆

pain [23] and complications warranting device removal, i.e. infection [24] or excessive migration [25]. Osteoblast adhesion and bony tissue mineralisation complicates the removal of plating systems, increasing removal torque, and predisposing screw damage and bone refracture [4, 26].

Osteoblast function and differentiation has recently been shown to be regulated to a high degree by adhesion and subsequent cellular spreading [27]. This study demonstrates the influence that nanoscale pits exert on cellular spreading and adhesion formation. Human osteoblasts spread well on smooth and 'Rand' substrates yet this spreading and adhesion formation was severely disrupted on 'Sq' substrates. Work to date suggests that adhesion formation is influenced by filopodial spatial gathering, and that pitted nanotopography disrupts the ability of fibroblasts to form cell-substrate interactions at the site of these pits [12, 28]

The high degree of order and regularity of the 'Sq' substrate was absent in the 'Rand' nanotopography, giving rise to relatively large areas of smooth 'PC' and to large compound pits. The absence of topographical modification at these areas of smooth PMMA may allow for cell adhesions to form, and thus aid intracellular tension, which in turn supports the formation of a well developed cytoskeleton and cell spreading. It can also be hypothesized that the large compound pits observed are also able to accommodate cellular extensions and facilitate adhesion formation, therefore increasing the area over which cell-substrate adhesion can occur.

S-phase cells have been shown to undergo increased spreading and have a reduced intercell variation in adhesion numbers [14, 29]. In this study cells were identified as being within S–phase by the incorporation of a thymidine analogue, BrdU into their total DNA. This strategy was adopted to ensure that any variation observed is indeed a result of interaction with nanotopography, rather than as a result of variation occurring as the cell progresses through the cell cycle. Cell spreading was reduced on the nanopitted substrates but the reason for this reduction may have several possible causes. It seems probable that the dimensions of the nanoscale pits prevent sufficient contact formation at the cell—substrate interface and hence disrupt early focal contact formation.

Adhesion formation was consistently observed to occur at the cell periphery in HOBs cultured on nanopit substrates, whereas adhesions were also noted in the perinuclear zone of cells on control substrates. Stress fibre formation and the terminating peripheral adhesions did not occur within lamellapodia of HOBs, rather, cytoplasmic actin and membrane ruffling was observed (Fig. 2). This observation suggests that focal adhesion formation is preceded by the active gathering of spatial information by integrin rich filopodial/lamellapodial extensions occurring at the leading edge, and that this perception plays a key role in the early adhesion development. This filopodial sensing has previously been reported by Dalby *et al*. to occur in fibroblasts cultured on 10 nm high polystyrene islands [30].

5 Conclusion

Nanopit topography disrupts adhesion formation in a manner dependant on pit symmetry and order. Highly ordered pits reduce cell spreading by inhibiting adhesion formation. This observation was supported by the increased HOB spreading and adhesion formation observed as nanopit conformations become more random. This data implements nanopit topography as a viable method to reduce osteoblast adhesion and may provide *in vivo* applications.

Acknowledgments This work was supported by a grant 04-D81 from the AO Research Fund, Switzerland. MJD is a BBSRC David Phillips Fellow, NG is a Royal Society of Edinburgh Research Fellow - they are supported through these fellowships. We would like to thank the following people: Prof Adam Curtis and Dr Mathis Riehle for their interesting discussion and support and John Pedersen (SDC Dandisc A/S, Denmark) for the organising and preparation of nickel shims.

References

1. H. LIAO, A. S. ANDERSSON, D. SUTHERLAND, S. PETRONIS, B. KASEMO, and P. THOMSEN, *Biomaterials* **24** (2003) 649.
2. G. CORDIOLI, Z. MAJZOUB, A. PIATTELLI and A. SCARANO, *Int J. Oral. Maxillofac Implants* **15** (2000) 668.
3. M. SUNDFELDT, L. V. CARLSSON, C. B. JOHANSSON, P. THOMSEN and C. GRETZER, *Acta. Orthop.* **77** (2006) 177.
4. P. L. SANDERSON, W. RYAN, and P. G. TURNER, *Injury* **23** (1992) 29.

5. R. D. OLESCHUK, M. E. MCCOMB, A. CHOW, W. ENS, K. G. STANDING, H. PERREAULT, Y. MAROIS and M. KING, *Biomaterials* **21** (2000) 1701.
6. A. D. BERSHADSKY, C. BALLESTREM, L. CARRAMUSA, Y. ZILBERMAN, B. GILQUIN, S. KHOCHBIN, A. Y. ALEXANDROVA, A. B. VERKHOVSKY, T. SHEMESH and M. M. KOZLOV, *Eur. J. Cell. Biol.* **85** (2006) 165.
7. E. ZAMIR and B. GEIGER, *J. Cell. Sci.* **114** (2001) 3583.
8. B. ZIMERMAN, T. VOLBERG, and B. GEIGER, *Cell. Motil. Cytoskeleton* **58** (2004) 143.
9. M. J. DALBY, S. J. YARWOOD, M. O. RIEHLE, H. J. JOHNSTONE, S. AFFROSSMAN and A. S. CURTIS, *Exp. Cell. Res.* **276** (2002) 1.
10. K. A. DIEHL, J. D. FOLEY, P. F. NEALEY and C. J. MURPHY, *J. Biomed. Mater. Res.* **A** (2005).
11. B. ZHU, Q. ZHANG, Q. LU, Y. XU, J. YIN, J. HU and Z. WANG, *Biomaterials* **25** (2004) 4215.
12. M. J. DALBY, N. GADEGAARD, M. O. RIEHLE, C. D. WILKINSON and A. S. CURTIS, *Int J. Biochem. Cell. Biol.* **36** (2004) 2005.
13. M. J. DALBY, S. CHILDS, M. O. RIEHLE, H. J. JOHNSTONE, S. AFFROSSMAN and A. S. CURTIS, *Biomaterials* **24** (2003) 927.
14. S. J. CROSS, I. *ap Gwynn, Cytobios* **50** (1987) 41.
15. N. GADEGAARD, S. THOMS, D. S. MACINTYRE, K. MCGHEE, J. GALLAGHER, B. CASEY and C. D. W. WILKINSON, *Microelectr. Eng.* **67–68** (2003) 126.
16. N. GADEGAARD, M. MOSLER and M. B. LARSEN, *Macromolecular Mater Eng.* **288** (2003) 76.
17. L. J. HEYDERMAN, H. SCHIFT, C. DAVID, J. GOBREACHT and T. SCHWEIZER, *Microelectr. Eng.* **54** (2000) 229.
18. R. S. PRATHER, A. C. BOQUEST and B. N. DAY, *Cloning* **1** (1999) 17.
19. V. GIRISH and A. VIJAYALAKSHMI, *Indian. J. Cancer.* **41** (2004) 47.
20. A. S. SANTIAGO, E. A. SANTOS, M. S. SADER, M. F. SANTIAGO and A. SOARES GDE, *Pesqui Odontol Bras* **19** (2005) 203.
21. M. MARCHISIO, M. DI CARMINE, R. PAGONE, A. PIATTELLI and S. MISCIA, *J. Biomed. Mater. Res. B Appl. Biomater.* **75** (2005) 251.
22. M. J. DALBY, M. O. RIEHLE, H. J. JOHNSTONE, S. AFFROSSMAN and A. S. CURTIS, *J. Biomed. Mater. Res.* **A 67** (2003) 1025.
23. O. L. BROWN, D. R. DIRSCHL and W. T. OBREMSKEY, *J. Orthop. Trauma.* **15** (2001) 271.
24. K. ISLAMOGLU, O. K. COSKUNFIRAT, G. TETIK and H. E. OZGENTAS, *Ann. Plast. Surg.* **48** (2002) 265.
25. M. H. BAUMS, B. A. ZELLE, W. SCHULTZ, T. ERNSTBERGER and H. M. KLINGER, *Knee. Surg.. Sports. Traumatol. Arthrosc.* (2006).
26. E. R. JAGO and C. J. HINDLEY, *Injury* **29** (1998) 439.
27. R. MCBEATH, D. M. PIRONE, C. M. NELSON, K. BHADRIRAJU and C. S. CHEN, *Dev. Cell.* **6** (2004) 483.
28. J. O. GALLAGHER, K. F. MCGHEE, C. D. WILKINSON and M. O. RIEHLE, *IEEE Trans. Nanobioscience* **1** (2002) 24.
29. D. O. MEREDITH, G. R. OWEN, I. AP GWYNN and R. G. RICHARDS, *Exp. Cell. Res.* **293** (2004) 58.
30. M. J. DALBY, M. O. RIEHLE, H. JOHNSTONE, S. AFFROSSMAN and A. S. CURTIS, *Cell. Biol. Int.* **28** (2004) 229.